

# NANOSTRUCTURED WEAR-RESISTANT COATINGS BASED ON REFRACTORY METALS NITRIDES: PHYSICAL-MECHANICAL PROPERTIES AND STRUCTURAL-PHASE STATE

Anton Panda<sup>1</sup>, Konstantyn Dyadyura<sup>2</sup>, Tatyana Hovorun<sup>2</sup>, Oleksandr Pylypenko<sup>2</sup>  
Marina Dunaeva<sup>2</sup>, Iveta Pandová<sup>1</sup>

<sup>1</sup> *Technical University of Kosice, Faculty of Manufacturing Technologies with a Seat in Presov, Slovakia*

<sup>2</sup> *Faculty of Technical Systems and Energy Efficient Technologies, Sumy State University, Ukraine*

## Corresponding author:

Anton Panda

Technical University of Kosice

Faculty of Manufacturing Technologies with a Seat in Presov

Bayerova1, 080 01 Prešov, Slovakia

phone: +421 55 602 6316

e-mail: anton.panda@tuke.sk

---

Received: 20 August 2018

Accepted: 14 September 2019

## ABSTRACT

Results of scientific researches show the trend of active using nitrides and borides of transition metals and their combination in developing protective materials. While single elements nitrides have been well studied, their multilayer modifications and combinations require more detailed study. Physical-mechanical properties and structural-phase state of multilayer coating according to the deposition conditions is an important task for the study. It will be the analysis of physical-mechanical and electrical properties of coatings based on refractory metals nitrides, their structure and phase composition and surface morphology depending on the parameters of condensation. It was established the structure and behavior of nano scale coatings based on refractory metals nitrides (Ti, Zr) depending on the size of nano grains, texture, stress occurring in coatings.

## KEYWORDS

nanocomposite coatings, friction, wear, hardness, multilayered TiN/ZrN coatings.

---

## Introduction

The development of theories and technologies in the field of new materials leads to an increase in the number of elements (components) and/or layers of metallic coatings. Recently, nitrides complexes covering element and phase composition are used more and more widely. In such surfaces, appropriate selection of components and concentrations of deposited or individual layers made it possible to improve a range of functional options [1–4].

The relationship of structure-phase state and functional properties of protective and/or wear-resistant coatings based on Ti, N, and Al was investigated in many works. Most of them, however, focused on the analysis of certain issues related to the problems of data acquisition on coatings [1–3]

and made only a partial analysis of their physical and electrical properties [4–7].

Increased interest in nitride coatings is conditioned by high hardness, melting point, chemical stability, high corrosion and resistance to wear [8]. Along with a number of benefits thick nitride coatings are characterized by high internal stresses, fragility, which leads to cracking and poor adhesion of coatings [9].

Over the past few years, several new material systems have been developed, including TiN NbN, TiN VN, CrN TiN, AlN TiN, and Ni TiN, CN TiN, which exhibit considerably higher hardness than individual components. Hardness greater than 50 GPa was observed for systems based on TiN NbN and TiN VN [10]. The metal based on multi-layer TiN/ZrN, with columnar morphology was investigated as a pro-

tective coating for saw blades for cutting [11]. In order to increase the performance of wear-resistant coatings for industrial applications, Ti or Zr/ZrN and TiN/ZrN multilayer coatings were applied to 12H18N9T steel substrates using two magnetron sputtering techniques.

## Experimental techniques

The coating was obtained by vacuum-arc deposition from two sources (targets). The first target was titanium grade BT-1-00 (Fe < 0.12%; C < 0.05%; Si < 0.08%; N < 0.04%; O < 0.1; H < 0.008; Ti was in the range 99.5–99.9), the second was zirconium (see pos. 1 in Fig. 1), obtained by electron-arc melting. A substrate of 12H18N9T steel with dimensions of 15 × 15 × 2.5 mm (roughness Ra = 0.09 microns) was used as a substrate for deposition of coatings. It was placed on sample holders (pos. 2 in Fig. 1). All devices for vacuum deposition are illustrated in Fig. 1. Precipitation occurred at PN = 3 · 10<sup>-3</sup> Torr and constant bias on the substrate was Us = -150 V. A mixture of gases N2+Ar, in a proportion of 1:10, was fed into the chamber through the tube (pos. 3 in Fig. 1).

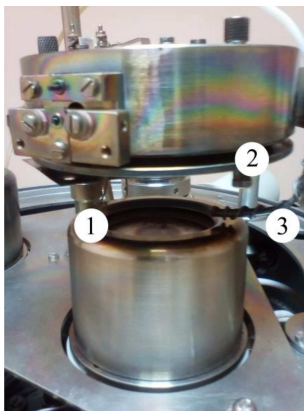


Fig. 1. Device for vacuum deposition: 1 – one of the targets; 2 – samples holder with the possibility of rotation; 3 – gas injection tube.

Three series of coatings were deposited that differed by the thickness of layers but had the same overall thickness. The thickness of the individual layers of the film system controlled by two methods: by quartz resonator (during condensation) and by optical interferometer (after condensation).

The first series of coatings had a thickness of a pair of layers (bilayer) TiN/ZrN  $\lambda \approx 40$  nm, the second series of coatings had a thickness (bilayer) TiN/ZrN with  $\lambda \approx 70$  nm, the third series of coatings had a thickness (bilayer) TiN/ZrN  $\lambda \approx 250$  nm.

The total thickness of the deposited coatings was –  $h \approx 14$  microns.

The study of the morphology of the samples is possible using a scanning electron microscope JEOL JSM –7000 F (Field Emission Scanning Electron Microscope) and EDX analysis in Institute of Materials Research of Kosice.

## Principles and methods of forming wear-resistant coatings

For the majority of polycrystalline materials, a typical increase of hardness and elastic limit with decreasing average size of crystallites (the Hall-Patch law) – is an example of mechanical side effects. Some of the physical most clearly visible side effects are the following: reduction of the melting temperature of nanomaterial compared to the volume as a result of an increasing value of surface energy, a sharp change of electric and magnetic properties. Among the existing principles of creating functional coatings for various purposes the most promising is the concept of multi-layer architecture coatings, such as coatings that are capable to meet contradictory requirements of different customers. Multiple tracks are supposed to be used to satisfy the conditions of simultaneous birth of islands of various mutually insoluble or soluble phases, limiting the growth centers of nucleus. The coating composition must contain plastic phases that carry out internal stress relaxation and growth inhibition of embryonic cracks. The multi-layer architecture makes it possible to create coverage, including both metastable and compound materials in a single geometric body, and thus makes it possible to combine different concepts of individual layers in a multilayer coating (Fig. 2).



Fig. 2. The model of multiple nano-composite coatings self-microstructure in infancy mutually insoluble phases [12].

According to the proposed design principles of coating, the method of forecasting their composition consists in selection of the items that provide many

phasing of coatings in terms of their synthesis procedure of forming a volume content of these phases and therefore little difference between the probability and possibility of formation of islets of relaxation stress concentrators within their communication.

With multilayered coatings of nanoscale thickness, each of its layers can be activated by different kinds of processes of energy absorption at optimal architecture, and structure of the coating increases the viscosity and strength of the coating only with a slight decrease in hardness (ensuring a balanced ratio of “hardness/viscosity”).

### Physical properties of wear-resistant coatings based on nitrides of refractory metals

The use of such methods of condensation as magnetron sputtering, ion deposition, and arc evaporation techniques, made it possible to obtain film and TiN coatings on various types of substrates with excellent adhesion and good reproducibility of durability and resistance to oxidation. The need for new materials with significantly improved properties regarding wear and corrosion contributed, however, to the search for new solid composite materials (e.g. Ti-Al-TiN, Ti-Zr-TiN, Ti-Al-Zr-TiN, and Ti-Al-VN) and it encouraged the study of their properties [13].

In particular, in the reference [14] showed that the coating  $\text{Ti}_{0.5}\text{Al}_{0.5}\text{N}$ , deposited on high-speed steel by magnetron sputtering had higher performance compared to TiN coatings deposited in solid form in terms of wear due to high resistance to oxidation at high temperatures. The reason for this is the formation of the protective layer, greatly enriched  $\text{Al}_2\text{O}_3$  that prevents rapid oxidation of the  $\text{Ti}_{0.5}\text{Al}_{0.5}\text{N}$  layer.

Comparison of micro-hardness (Ti, Al)N and (Ti, Zr)N films deposited on the substrates SS-304 under various conditions of deposition was carried out in [15]. It was noted that micro-hardness (Ti, Al)N films increased with the magnitude of the negative voltage applied to the substrate and N content in the system.

In the case of films (Ti, Zr)N, the authors observed the systematic changes with the change of micro-hardness as a result of a voltage applied to the substrate. Films deposited at a voltage of  $-50$  V had the lowest levels of hardness, but those deposited at  $-100$  V had the highest hardness at all flow rates of nitrogen. Besides, in contrast to the case of (Ti, Al)N films, micro-hardness films (Ti, Zr)N did not substantially depend on N content in films. However, it was found that micro-hardness films of similar

thickness ( $h \approx 1 \mu\text{m}$ ), regardless of the mode of deposition, increased with the decreasing Zr content in the films.

Comparison of the nano-hardness coating (Ti, Zr)N with the coatings deposited under equivalent conditions involved in the formation of a solid solution was performed by the authors [16]. Coating (Ti, Zr)N demonstrates significantly higher values of nano-hardness compared to TiN and ZrN. Nano-hardness of (Ti, Zr)N coatings depends on the applied bias voltage. Nanohardness of pure TiN and ZrN films is 18.1 and 2.3 GPa, respectively, while the hardness of (Ti, Zr)N film is close to 40 GPa.

Comparison of two series of the hardness of AlN/TiN and AlN/ZrN coatings depending on the period was studied by authors in [17]. Since the thickness of coatings was less than 2 nm, 25 g load generated on the indenter enables the penetration depth of the film of 0.3–0.5 microns. Thus, the hardness values measured were in comparison to the estimated values lower by 30–50 % than the actual hardness of the film due to the influence of the film thickness and soft lining. For films AlN/TiN with a thickness of  $\lambda = 1.4$  nm and  $\lambda = 3.6$  nm the hardness was approx. 21 GPa, for films with  $\lambda = 3.2, 2, 1$  and 1.8 nanometers of the hardness was more than 27 GPa. The hardness of AlN/ZrN coatings was generally lower than for AlN/TiN. The hardness of AlN/ZrN with  $\lambda = 4.8$  nm was below 20 GPa, for  $\lambda = 7.5$  nm – 24 GPa and  $\lambda = 16$  nm – 22 GPa [17].

Figure 3 shows firmness depending on the bias voltage on the substrate films AlN/TiN and AlN/ZrN, at a thickness of  $\lambda = 2\text{--}3$  nm. Dependence shows an increase in hardness with an increasing bias voltage for both series of films. The maximum hardness of 31 GPa was achieved with an offset voltage  $U_s = -100$  V, and the system AlN/TiN was highly textured along the (111) direction. For AlN/ZrN films, their structure is amorphous, and the maximum hardness reaches only approx. 20 GPa and it increases with an increasing bias voltage to the substrate, repeating the results for the coatings (Ti, Al)N and (Ti, Zr)N.

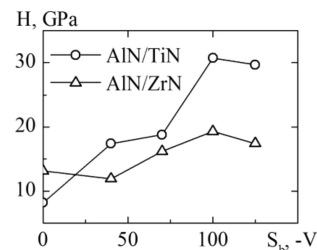


Fig. 3. Hardness of AlN/TiN and AlN/ZrN nanolaminate samples vs substrate bias voltage [14].

Mechanical properties of coatings [TiN/ZrN]N depending on the number of repetitions have been identified by nanoindentation measurements [18]. We can estimate the increase in hardness (H) and elastic modulus (Er), with the number of bilayers. The hardness is increased from  $15 \pm 1$  GPa to  $29 \pm 2$  GPa. The elastic modulus (Er) varies from  $180 \pm 1$  GPa to  $245 \pm 2$  GPa. The increase is approximately from 93 % to 36 % of hardness and elasticity module. The modulus increases with the number of bilayers in the coating. We can say that flexibility of multilayer structure is improved by increasing the number of bilayers. This behavior can be connected to the improved growth of solid surfaces using multilayer materials. This improvement led to a reduction in the size of grains observed with AFM image and it causes an increase in density for hard coating and produces a bias to break the blockade [19, 20].

Thus, analysis of the literature shows the promising use of multilayer coatings, where layers are composed of nitrides of refractory metals and have a layer thickness of approx. 20 - 30 nm, to improve the mechanical properties [21, 22]. Surface consisting of refractory metal nitride bilayer which is recurring, is characterized by high hardness, because the tension created in layers during the deposition, resists the dislocation motion.

The research shows that nano-hardness in multilayers TiN/ZrN increases with the decreasing modulation period  $\lambda$  (Table 1). This is consistent with previous studies, for example, for  $\lambda = 7.5$  nm, where the hardness of TiN/CrN film is 40 GPa [23]. This effect is strengthening with the decreasing  $\lambda$  and it can be connected both with grain size and a large number of interface layers (dislocation blocking and strain effects) [24]. It was found that Young's modulus in the range of multilayer coatings was between the values for the TiN (286 GPa) and the values for ZrN (349 GPa). It was established that Young's modulus decreased with the decreasing modulation period  $\lambda$ .

Table 1  
Hardness properties of the multilayer TiN/ZrN coatings.

Coated samples	Hardness		
	[HV] Micro-hardness	[HRA] Rockwell hardness A	[HRB] Rockwell hardness B
TiN/ZrN 534 layers	221.7	59.8	97.83
TiN/ZrN 134 layers ( $\lambda = 71$ )	202.0	57.55	94.25

The hardness of coatings determined by micro identification was the following: for  $\lambda \approx 40$  – H  $\approx$  42 GPa,  $\lambda \approx 70$  nm – H  $\approx$  38 GPa,  $\lambda \approx 250$  nm

– H  $\approx$  36 GPa. Thus, for all thicknesses the bilayer system TiN/ZrN is a typical high-solid state, making such coatings promising for use as protective wear-resistant materials.

The mechanism of increasing hardness is due to blocking intermediate layers of dislocations on the boundaries and inside the layers. This, in turn, is the result of differences in the composition of layers, of the significant disparity between the layers of crystalline structure, and of the presence of grain boundaries and defects in the layers.

Another possible mechanism for increasing the hardness of multilayers of nanometer scale can be explained by the Koehler model [25]. It is assumed that the increase in strength can be achieved in epitaxial hetero-structures consisting of layers with a thickness of few nanometers made of two metals A and B with high and low shear modulus, respectively. Dislocations are formed only in the metal B, which has a lower shear modulus. When the voltage (pressure – stress) is applied, they will interfere with cross interface B/A due to the repulsive force in the model A. The Koehler model was experimentally tested on different systems studied in the literature, such as epitaxial hetero-structures TiN/VN [26], TiN/NbN [27].

### Phase state and structure of coatings based on nitrides of refractory metals

Energy dispersive spectra, typical for all series of the coatings and characterizing their stoichiometry, are presented in Fig. 4. Radiographic studies of the samples show that after deposition in the surface layers (depth information layer of approx. 4  $\mu$ m) the

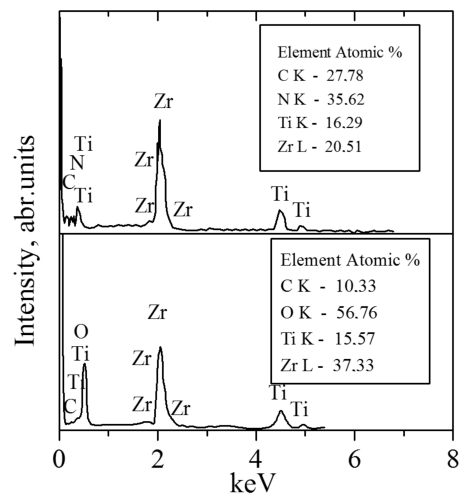


Fig. 4. EDX spectra and elemental composition TiN/ZrN coatings defined by them:  $\lambda \approx 70$  nm (top),  $\lambda \approx 250$  nm (bottom).

layers are formed, consisting of TiN and ZrN phases with cubic (structure type NaCl) crystal lattice without clearly expressed orientation of crystallites (grains). Figure 5 shows the characteristic X-ray fragment of the samples of multilayer coatings with different thickness  $\lambda$  period in bilayers. The increase of the thickness from  $\lambda \approx 70$  nm to  $\lambda \approx 250$  nm shows a slight increase in the deposit layers of TiN, which appears to change the intensity ratio of peaks and TiN-, ZrN-phase. Those research were executed together with the authors [2].

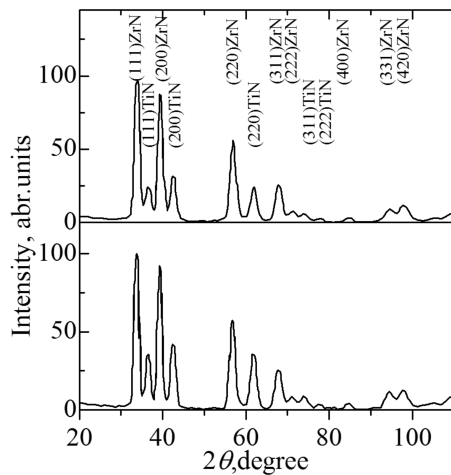


Fig. 5. X-ray diffraction spectra of coatings:  $\lambda \approx 70$  nm (top),  $\lambda \approx 250$  nm (bottom).

The increase of the deposition time, and with it also of the thickness of the layers and the total period of the multilayer system, leads to a change of the period of nitride crystal lattice phase in the layers. For TiN, phase grating period decreases with the increase of the thickness from 0.42415 nm for  $\lambda \approx 70$  nm (layer deposition time 20 seconds) to 0.4238800 nm for  $\lambda \approx 250$  nm (deposition time 40 seconds). The changes for ZrN are not so significant: from 0.4581055 nm for  $\lambda \approx 70$  nm to 0.4581046 nm for  $\lambda \approx 250$ . High integrity and lack of uniformity in the form of droplet phase that appears on the surface is also characteristic for this coating (Fig. 6).

Use of the scanning electron microscopy enabled a detailed analysis of deposited coatings. Figure 7 shows a lateral boundary surfaces at different magnification. We see that even on the majority of coatings the layers show a good uniformity of deposition.

Research conducted for the laminated structure of the ZrN/TiN bilayer with an increased thickness of the layers to 100 nm showed the changing nature of the growth surfaces. The dropping phase a good lamination and coating uniformity of deposition layers structure.

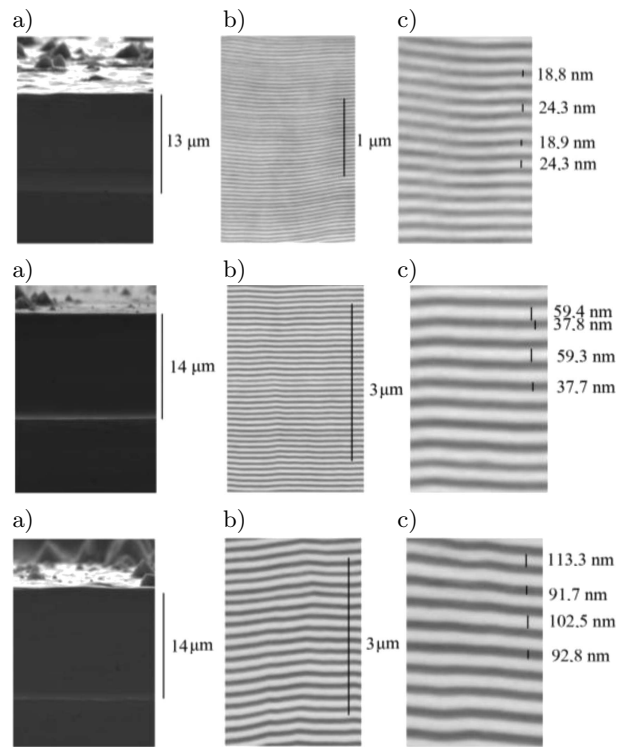


Fig. 6. SEM micrographs for ZrN/TiN bilayer (a) in the cross-section view of the number of layers 533, 233, and 134; and a general view of cleavage design; (b), (c) – enlarged fragments of the lateral surface coatings.

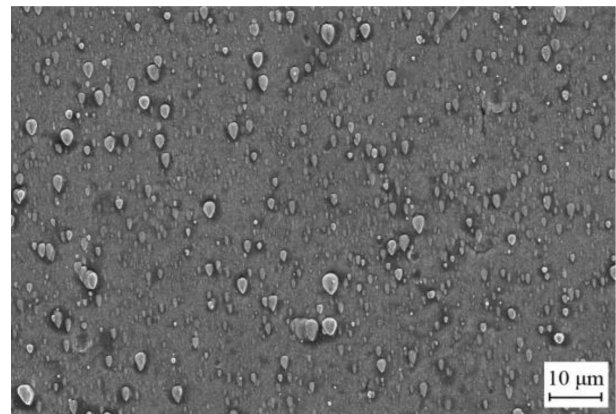


Fig. 7. Typical image of surface of the sample ZrN/TiN.

The individual layers (TiN dark, ZrN light) have a thickness of 100 nm columnar morphology growth. The average diameter of the column is approx. 500 nm (Fig. 7). SEM image of the surface in Fig. 6 shows sufficient free volume between column for precipitation of the coolant, thus indicating the possibility of improving the binding lubricant coat in triathl logical contact, which correlates very well with the result given in [28].

## Conclusions

It has been found that the structure, phase composition, texture, microstructure and surface roughness, and therefore the properties of hardness, were closely related to the composition of the target, to the size of the negative voltage applied to the substrate, to the gas mixture ratio, and to the power sputtering target. Our previous research has shown the promising application of multilayer coatings, where layers composed of nitrides of refractory metals with a layer thickness of approx. 20 - 30 nm, could improve the mechanical characteristics. Optimal parameters of nitride coating hardness are shown at a high negative voltage applied to the substrate. During the work, a series of coatings TiN/ZrN and (Ti,Zr)N was obtained. The research was focused on their composition and on their mechanical properties. It was determined that TiN/ZrN and (Ti,Zr)N coatings had columnar microstructure with preferred orientation (111). TiN/ZrN coatings had good continuity and lack of uniformity in volume and consisted of TiN and ZrN layers with a cubic structure. Increasing the thickness of the coating TiN/ZrN, condensed at the action of  $U_s = -100$  V, leads to a transition of the axis preferred orientation (111) to a non-textured state.

During research, we established that the highest hardness (42 GPa) and the smallest abrasive wear coating was inherent to the system of TiN/ZrN layers with the smallest thickness (20 nm) in the bilayer. We consider that this is the result of the influence of the grain size factor for each of the layers, which very appear in interphase boundaries, for such a system.

Thus, the technology, in which coating derived from an alternate and simultaneous electron bombardment by ion plasma flow of Ti and Zr, in an atmosphere of N gas, provided a surface that could be attributed to the class of extra hard materials.

*The authors would like to thank the KEGA grant agency for supporting their research work and for financing the project KEGA: 004TUKE-4/2017.*

## References

- [1] Pogrebnjak A.D., Dyadyura K.O., Gaponova O.P., *Features of thermodynamic processes on contact surfaces of multicomponent nanocomposite coatings with hierarchical and adaptive behaviour*, Metallofiz. Noveishie Tekhnol., 37, 7, 899–919, 2015, <http://mfint.imp.kiev.ua/ru/abstract/v37/i07/08-99.html>.
- [2] Pogrebnjak A.D., Ivasishin O.M., Beresnev V.M., *Arc-Evaporated Nanoscale Multilayer Nitride-Based Coatings for Protection Against Wear, Corrosion, and Oxidation*, Usp. Fiz. Met., 17, 1, 1–28, 2016, <https://doi.org/10.15407/ufm.17.01.001>.
- [3] Musil J., *Physical and mechanical properties of hard nanocomposite films prepared by reactive magnetron sputtering*, Chapter 10 in the book “Nanostructured Hard Coatings”, 2005, Springer Science + Business Media, LCC, New York, NY 10013, U.S.A., 407–463.
- [4] Samuelsson M., Lundin D., Jensen J., Raadu M.A., Gudmundsson J.T., Helmersson U., *On the film density using high power impulse magnetron sputtering*, Surf. Coat. Technol., 202, 2, 591, 2010, <https://doi.org/10.1016/j.surfcoat.2010.07.041>.
- [5] Hovorun T.P., Pylypenko O.V., Hovorun M.V., Dyadyura K.O., *Methods of Obtaining and Properties of Wear-resistant Coatings Based on Ti and N and Ti, Al and N*, J. Nano- Electron. Phys., 9, 2, 02026(7pp), 2017, [https://doi.org/10.21272/jnep.9\(2\).02026](https://doi.org/10.21272/jnep.9(2).02026).
- [6] Magnus F., Ingason A.S., Sveinsson O.B., Olafsson S., Gudmundsson J.T., *Morphology of TiN thin films grown on SiO<sub>2</sub> by reactive high power impulse magnetron sputtering*, Thin Solid Films, 520, 5, 1621, 2011, <https://doi.org/10.1016/j.tsf.2011.07.041>.
- [7] Vereshchaka A.A., Vereshchaka A.S., Mgaloblishvili O., Morgan M.N., Batako A.D., *Nano-scale multilayered-composite coatings for the cutting tools*, International Journal of Advanced Manufacturing Technology, Springer-Verlag, 72, 1–4, 1–15, 2014, <https://doi.org/10.1007/s00170-014-5673-2>.
- [8] Anders A., *Metal Plasmas for the Fabrication of Nanostructures*, Journ. Phys. Appl. Phys., 40, 2272, 2007, <https://doi.org/10.1088/0022-3727/40/8/S06>.
- [9] Straumal B.B., Vershinin N.F., Asrian A.A., Rabkin E., Kroeger R., *Nanostructured Vacuum Arc Deposited Titanium coatings*, Mater. Phys. Mech., 5, 39, 2002, <http://www.ipme.ru/e-journals/MPM/no.1502/straumal/straumal.pdf>.
- [10] Wong M.-S., Hsiao G.-Y., Yang Sh.-Yu, *Preparation and characterization of AlN/ZrN and AlN/TiN nanolaminate coatings*, Surf. Coat. Technol., 133–134, 160–165, 2000, [https://doi.org/10.1016/S0257-8972\(00\)00958-0](https://doi.org/10.1016/S0257-8972(00)00958-0).
- [11] Ulricha S., Ziebert C., Stqber M., Nold E., Holleck H., Gfken M., Schweitzer E., Schlogmacher P., *Correlation between constitution, properties and machining performance of TiN/ZrN multilayers*, Surf. Coat. Technol., 188–189, 331–337, 2004, <https://doi.org/10.1016/j.surfcoat.2004.08.056>.
- [12] Barshilia H.C., Acharya S., Ghosh M., *Performance evaluation of TiAlCrYN nanocomposite coatings deposited using four-cathode reactive unbalanced pulsed direct current magnetron sputtering system*,

- Vacuum., 85, 411, 2010, <https://doi.org/10.1016/j.vacuum.2010.08.003>.
- [13] Kovalev A., Wainstein D., Rashkovskiy A., *Investigation of anomalous physical properties of multilayer nanolaminate (TiAl)N/Cu coatings by electron spectroscopy techniques*, Surface and Interface Analysis, 42, 6–7, 1361–1363, 2010, <https://doi.org/10.1002/sia.3290>.
- [14] Gago R., Soldera F., Hübner R. et al., *X-ray absorption near-edge structure of hexagonal ternary phases in sputter-deposited TiAlN films*, Journal of Alloys and Compounds, 561, 87–94, 2013, <https://doi.org/10.1016/j.jallcom.2013.01.130>.
- [15] Meng Q., Wen M., Liu P., Zhang K., Zheng W., *Correlation between interfacial electronic structure and mechanical properties of ZrN/SiNx films*, Mater. Lett., 94, 61, 2013, <https://doi.org/10.1016/j.matlett.2012.12.011>.
- [16] Gassner G., Mayrhofer Ph., Kutschey K., Mitterer C., Kathrei M., *Magnéli phase formation of PVD Mo-N and W-N coatings*, Surf. Coat. Technol., 201, 3335, 2006, <https://doi.org/10.1016/j.surfcoat.2006.07.067>.
- [17] Svito I.A., Fedotova J.A., Miloslavljjevic M., Zhukowski P., Koltunowicz N.T., Saad A., Kierczynski K., Fedotov A.K., *Influence of sputtering atmosphere on hopping conductance in granular nanocomposite (FeCoZr)<sub>x</sub>(Al<sub>2</sub>O<sub>3</sub>)<sub>1-x</sub> films*, J. Alloys Compd., 615, 1, S344, 2014, <https://doi.org/10.1016/j.jallcom.2013.12.061>.
- [18] Koltunowicz T.N., Zhukowski P., Bondariev V., Saad A., Fedotova J.A., Fedotov A.K., Miloslavljjevic M., Kasiuk J.V., *Enhancement of negative capacitance effect in (CoFeZr)<sub>x</sub>(CaF<sub>2</sub>)<sub>(100-x)</sub> nanocomposite films deposited by ion beam sputtering in argon and oxygen atmosphere*, J. Alloys Compd., 615, 1, S361, 2014, <https://doi.org/10.1016/j.jallcom.2013.12.125>.
- [19] Braic M., Braic V., Balaceanu M., Pavelescu G., Vladescu A., *Plasma deposition of alternate TiN/ZrN multilayer hard coatings*, J. Optoelectron. Adv. Mater., 5, 1399–1404, 2003, <http://citeseerx.ist.psu.edu/viewdoc/download?doi=10.1.1.556.7277&rep=rep1&type=pdf>.
- [20] Poliak N.I., Anishchik V.M., Valko N.G., Karwat C., Kozak C., Opielak M., *Mechanical Properties of Zn-Ni-SiO<sub>2</sub> Coating Deposited under X-ray Irradiation*, Acta Phys. Pol. A., 125, 6, 1415, 2014, 10.12693/APhysPolA.125.1415.
- [21] Abadias G., Michel A., Tromas C., Jaouen C., Dub S.N., *Stress, interfacial effects and mechanical properties of nanoscale multilayered coatings*, Surf. Coat. Technol., 202, 844–853, 2007, <https://doi.org/10.1016/j.surfcoat.2007.05.068>.
- [22] Chen S.-F., Kuo Y.-C., Wang C.-J., Huang S.-H., Lee J.-W., Chan Y.-C., Chen H.-W., Duh J.-G., Hsieh T.-E., *The effect of Cr/Zr chemical composition ratios on the mechanical properties of CrN/ZrN multilayered coatings deposited by cathodic arc deposition system*, Surf. Coat. Technol., 231, 247–252, 2013, <https://doi.org/10.1016/j.surfcoat.2012.03.002>.
- [23] Musil J., Novak P., Hromadka M., Cerstvy R., Soukup Z., Savkova J., *Mechanical and tribological properties of sputtered Mo-O-N coatings*, Surf. Coat. Technol., 215, 386, 2013, <https://doi.org/10.1016/j.surfcoat.2012.06.090>.
- [24] Martev I.N., Dechev D.A., Ivano N.P., Uzunov Ts.D., Kashchieva E.P., *Nanolaminated TiN/Mo<sub>2</sub>N hard multilayer coatings*, J. Phys. Conf. Ser., 223, 1, 012, 2010, <https://doi.org/10.1088/1742-6596/223/1/012019>.
- [25] Kazdaev K.R., Abylkalykova R.B., Kveglis L.I., *Regularities of Formation of the Ordered Structures in Molybdenum at Ion Implantation*, J. Sib. Fed. Univ. Eng. Technol., 5, 560, 2012, [http://elib.sfu-kras.ru/bitstream/2311/3198/1/09\\_Kazdaev.pdf](http://elib.sfu-kras.ru/bitstream/2311/3198/1/09_Kazdaev.pdf).
- [26] Yen H.W., Huang C.Y., Yang J.R., *Characterization of interphase-precipitated nanometer-sized carbides in a Ti-Mo-bearing steel*, Scr. Mater., 61, 616, 2009, <https://doi.org/10.1016/j.scriptamat.2009.05.036>.
- [27] Machon D., Daisenberger D., Soignard E., Shen E., Kawashima T., Takayama-Muromachi E., McMillan P.F., *High pressure – high temperature studies and reactivity of  $\gamma$ -Mo<sub>2</sub>N and  $\delta$ -MoN*, Phys. Stat. Solid. A. 2006, 203, 5, 831, 2006, <https://doi.org/10.1002/pssa.200521008>.
- [28] Zhang G., Tianxiang F., Tao W., Hailin C., *Microstructure, mechanical and tribological behavior of MoNx/SiNx multilayer coatings prepared by magnetron sputtering*, Appl. Surf. Sci., 274, 231, 2013, <https://doi.org/10.1016/j.apsusc.2013.03.021>.
- [29] Panda A., Duplak J., Jurko J. et al., *New experimental expression of durability dependence for ceramic cutting tool*, International Conference on Applied Mechanics and Materials (ICAMM 2012) Location: Sanya, PEOPLES R CHINA Date: Nov 24–25, 2012, Applied Mechanics and Materials I, PTS 1–3 Book Series: Applied Mechanics and Materials, 275–277, 2230–2236.
- [30] Jurko J., Dzuwon M., Panda A. et al., *Deformation of material under the machined surface in the manufacture of drilling holes in austenitic stainless steel*, 8th International Scientific – Technical Conference of Material Engineering Practice, Chemicke Listy, 105, SI, Supplement: 4, S600–S602, 2011.
- [31] Panda A., Duplak J., Jurko J., *Analytical expression of T-v(c) dependence in standard ISO 3685 for cutting ceramic*, International Conference on Materials Engineering for Advanced Technologies (ICMEAT2011), Singapore, Materials Engineering for Advanced Technologies, PTS 1 and 2 Book Series: Key Engineering Materials, 480–481, 317–322, 2011.